Modulator-Free Variable Multi-Rate FSO Communication 1 km Outfield Demonstration Based on Chirp-Managed Laser

Zhuang Xie, Shuaiwei Jia, Wen Shao, Yang Wang, Rong Ma, Sentao Wei, Peixuan Liao, Dongquan Zhang, Weiqiang Wang, Duorui Gao, Wei Wang, and Xiaoping Xie

***Abstract*—Due to the high energy efficiency per bit and high sensitivity, Return-to-zero differential-phase-shift-keying (RZ-DPSK) is perfectly suitable for free-space laser communications. However, the conventional generation method of RZ-DPSK optical signal requires two modulators, which is costly, bulky, and heavy, significantly hindering the application of RZ-DPSK in size, weight, and power (SWaP)-constrained satellite platforms. In this paper, we propose and experimentally demonstrate a modulator-free variable multi-rate RZ-DPSK free-space optical (FSO) communication system based on chirp-managed laser (CML). Based on the proposed scheme, an FSO outfield experiment over 1 km has been successfully undertaken, achieving receiving sensitivities of −48.9 dBm and −45.6 dBm at 2.5 Gbps and 5 Gbps, with bit error rate (BER) of 1×10^{-3} without forward error correction (FEC), respectively. The performance of the proposed system is also investigated by studying the eye diagrams under two different test conditions of back-to-back transmission and 1-km free space transmission. In addition to the small size, lightweight and low cost, the proposed scheme shows great potential for a variety of FSO communication applications ranging from Cube-Star to larger satellite laser communication platforms.**

***Index Terms*—Free-space optical communication, modulator-free, miniaturization, variable multi-rate.**

Manuscript received 8 September 2022; revised 25 September 2022; accepted 28 September 2022. Date of publication 3 October 2022; date of current version 17 October 2022. This work was supported in part by the National Natural Science Foundation of China under Grants 61231012 and 91638101, and in part by the National Key Research and Development Program of China under Grant 2018YFC0307904-02. *(Zhuang Xie and Shuaiwei Jia contributed equally to this work.) (Corresponding authors: Duorui Gao; Xiaoping Xie.)*

Zhuang Xie, Shuaiwei Jia, Wen Shao, Yang Wang, and Xiaoping Xie are with the State Key Laboratory of Transient Optics and Photonics, Xi'an Institute of Optics and Precision Mechanics, Chinese Academy of Sciences, Xi'an 710119, China, with the School of Future Technology, University of Chinese Academy of Sciences, Beijing 100049, China, and also with University of Chinese Academy of Sciences, Beijing 100049, China (e-mail: xiezhuang@opt.ac.cn; jiashuaiwei@opt.cn; shaowen@opt.cn; wangyang2017@opt.cn; xxp@opt.ac.cn).

Rong Ma, Peixuan Liao, and Duorui Gao are with the State Key Laboratory of Transient Optics and Photonics, Xi'an Institute of Optics and Precision Mechanics, Chinese Academy of Sciences, Xi'an 710119, China, and also with University of Chinese Academy of Sciences, Beijing 100049, China (e-mail: tyutmarong@163.com; liaopeixuan@opt.cn; gaoduorui@opt.ac.cn).

Sentao Wei, Dongquan Zhang, Weiqiang Wang, and Wei Wang are with the State Key Laboratory of Transient Optics and Photonics, Xi'an Institute of Optics and Precision Mechanics, Chinese Academy of Sciences, Xi'an 710119, China (e-mail: weisentao@opt.ac.cn; zhangdongquan@opt.ac.cn; wwq@opt.ac.cn; wangwei2012@opt.ac.cn).

Digital Object Identifier 10.1109/JPHOT.2022.3211268

I. Introduction

With the massive application of multiple high-resolution earth-observing sensors, the demand for transmission bandwidth of satellites and aircraft has risen sharply over the past few years [1]. Neither traditional radio frequency (RF) communication nor classical data compression technology can cope with the challenge of transmitting this huge amount of data to the ground [2]. However, owing to the advantages of large bandwidth, free-space optical (FSO) communication is expected to break through this limitation and can provide high-speed, flexible and efficient communication links between satellites and the ground [3], [4], [5].

At present, FSO communications are widely carried out in many countries and organizations around the world, such as NASA's laser communications relay demonstration (LCRD), ESA's European data relay satellite system (EDRS) and JAXA's Japanese optical data relay system (JDRS) and so on. These projects mostly use binary phase-shift keying (BPSK) or differential phase-shift keying (DPSK) modulation format at a fixed transmission power and a fixed communication rate [6], [7], [8], [9], [10], and the latter has attracted wide attention due to its relatively simple design, well-known high sensitivity and high reliability. To generate the desired DPSK modulation format, a typical transmitter consists of a laser and an external Mach-Zehnder modulator (MZM), which makes it prohibitively bulky, heavy and costly for SWaP-limited satellite platforms. This problem is even more serious for high sensitivity RZ-DPSK modulation formats that require two MZMs to generate, and greatly increases system complexity. In addition, to ensure the normal operation of laser communication links, the laser communication systems usually maintain a certain margin of received power, which can be detrimental to power-constrained free-space platforms such as power-starved satellites. Fortunately, the variable multi-rate laser communication system can realize the reasonable exploitation of power resources in power-constrained mobile platforms by adjusting the communication rate according to the link loss. Thus, there is an urgent requirement for laser communication systems that are miniaturized and can generate arbitrary rates. Owing to the special chirp characteristics of chirp-managed laser (CML), CML can generate phase-modulated signals in response to the input electrical-level signal and have a small footprint [11],

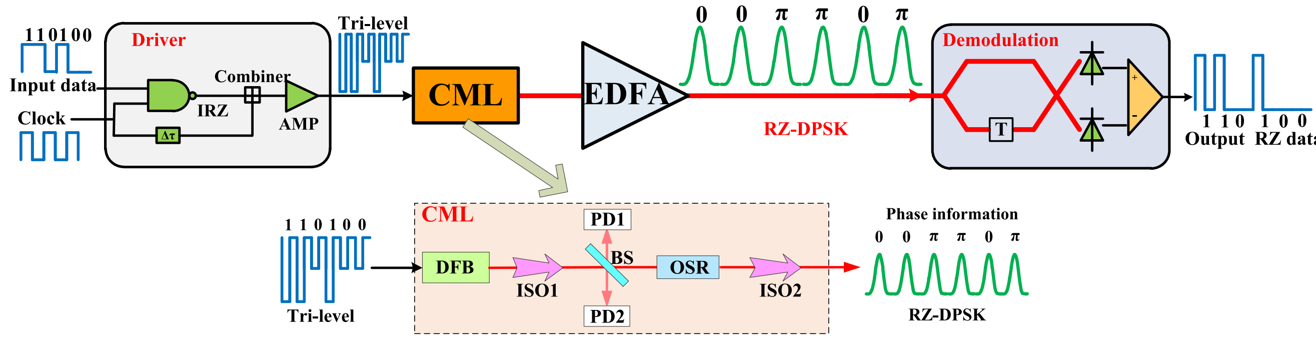

Fig. 1. Process of the operation of the CML-based modulator-free variable multi-rate RZ-DPSK FSO communication system. Insets show the basic structure of CML. DFB: distributed feedback laser, TEC: thermo electric cooler, ISO: isolator, BS: beam splitter; OSR: optical spectrum re-shaper; PD: photodetector.

[12], [13], [14], [15], [16]. These advantages give the CML a great potential for free-space applications.

In this paper, a CML-based modulator-free variable multi-rate RZ-DPSK FSO communication system is proposed and demonstrated. Firstly, we convert the original data into a tri-level signal, and then the CML generates the RZ-DPSK signal based on the chirp effect caused by the tri-level signal jump. Meanwhile, we successfully carried out an outfield experiment between two buildings 1 km apart to evaluate the communication performance of the FSO communication system. The experimental results show that the receiving sensitivity is −48.9 dBm and −45.6 dBm at 2.5 Gbps and 5 Gbps, with the bit error rate (BER) of 1×10^{-3}, respectively. In addition, the quality of the generated RZ-DPSK signal and the performance of the proposed system are analyzed and discussed. The proposed scheme is not only small size, lightweight and cost-efficient, but also can establish flexible and efficient transmission links in a large dynamic range of power, providing an optional solution for FSO communication, especially for satellites and space vehicles.

II. Operation Principles

Fig. 1 shows the communication process of the proposed system. The raw data is pre-encoded by the driver to generate a tri-level electrical signal which drives the CML. The CML generates the RZ-DPSK optical signal by subtly utilizing the chirp effect caused by electrical signal jumps. At the receiver terminal, demodulation of the RZ-DPSK optical signal is done optically using a spatial structure Mach-Zehnder interferometer (MZI) with a one-bit delay in one arm, followed by a balanced photoreceiver to output RZ data. The inset of Fig. 1 shows the basic structure of CML. The CML mainly consists of two components, a distributed feedback laser (DFB) and a co-packaged optical spectrum re-shaper (OSR). OSR converts the nonlinear chirped wave from DFB laser into a square wave with adiabatic chirp that has a consistent phase over a pulse, and can improve the extinction ratio when generating intensity signals [15]. In this study, we utilize the adiabatic chirp characteristic of the CML to accomplish phase modulation without modulators, which essentially changes the frequency of the optical carrier. The variation of phase $\Delta\phi$ can be obtained by integrating the frequency shift Δf caused by the adiabatic chirp against time

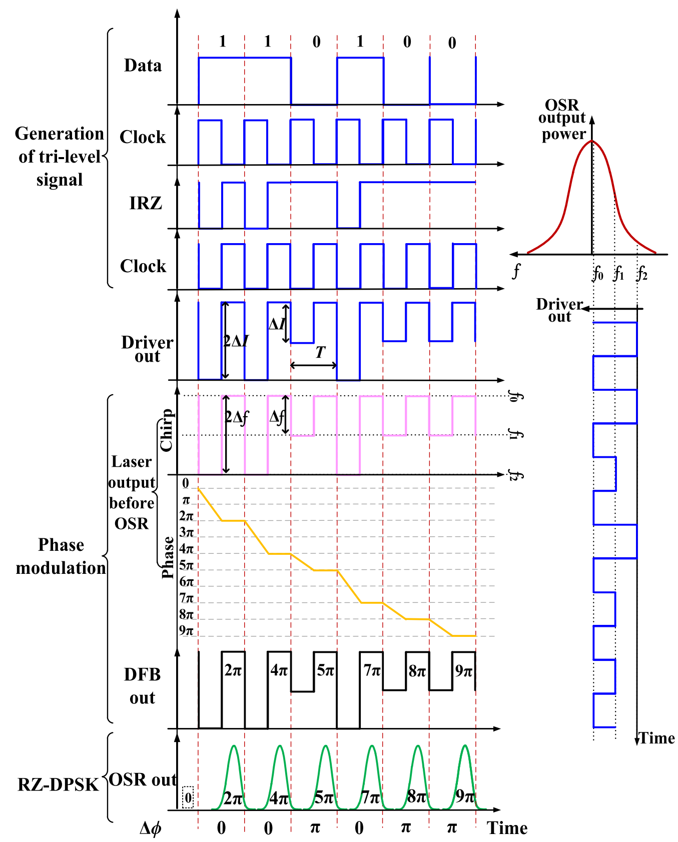

Fig. 2. Schematic of the CML generating RZ-DPSK modulation format.

[14], which is given by

$$\Delta\phi = 2\pi \int_0^{T/2} \Delta f\,(t)dt \tag{1}$$

where T is the 1-bit time of the modulation rate. In this way, the phase-modulated signal can be generated by controlling the frequency shift of the CML.

For the RZ-DPSK modulation format, the CML requires a tri-level drive waveform. Taking "110100" as an example, Fig. 2 illustrates in detail the working principle of the CML for generating RZ-DPSK signals through the generation of tri-level

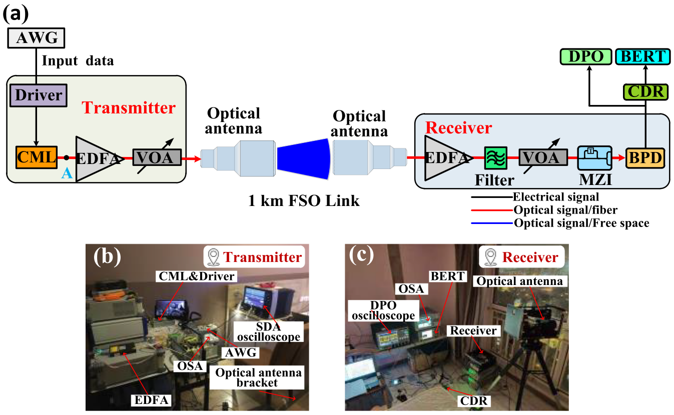

Fig. 3. (a) Schematic setup of the CML-based modulator-free variable multi-rate RZ-DPSK FSO communication system. (b) Experiment configuration at the transmitter terminal. (c) Experiment configuration at the receiver terminal.

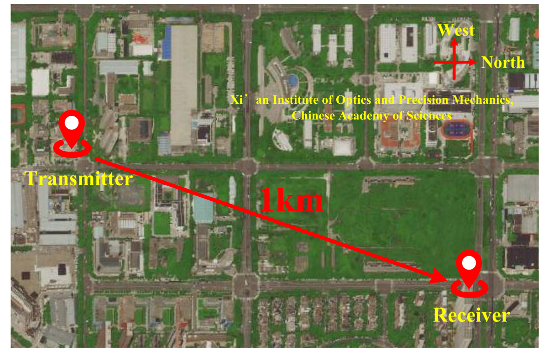

Fig. 4. Location of the transmitter and the receiver.

electrical signals and phase modulation. Firstly, the non-return-to-zero (NRZ) "110100" raw pulse signal does NAND operation with a synchronous clock signal to generate an inverse RZ (IRZ) signal with 50% duty cycles, and then the IRZ signal is summed with the delayed half-bit clock signal to produce a tri-level electrical signal, which is amplified to drive the CML. Note that the tri-level electrical signal changes with the input signals 1 and 0, respectively causing $2\Delta I$ and ΔI changes in the driving current of the CML, and this action occurs only within half a bit cycle. The amount of change in the drive current of $2\Delta I$ and ΔI causes the adiabatic chirp of the CML $2 \times \Delta f = 2/T$ and $\Delta f = 1/T$, respectively. Then, according to Eq. (1), the carrier phase shifts corresponding to $2\Delta I$ and ΔI are

$$\begin{cases} \Delta\phi_{2\Delta I} = 2\pi \times \frac{T}{2} \times \frac{2}{T} = 2\pi \\ \Delta\phi_{\Delta I} = 2\pi \times \frac{T}{2} \times \frac{1}{T} = \pi \end{cases}, \quad (2)$$

thereby completing the phase modulation of signals 1 and 0. In this case, the desired RZ-DPSK signal is obtained by adjusting the OSR to suppress f_1 and f_2 frequency corresponding to two low-level of tri-level signals and pass f_0 corresponding to high-level of tri-level signals. For the generation of variable multi-rate RZ-DPSK optical signals, the transmission rate of the raw data needs to be adjusted. That is, the rate of the RZ-DPSK optical signal follows the transmission rate of the raw data.

III. Experimental Setup

Fig. 3 shows the outfield experiment setup of a modulator-free variable multi-rate RZ-DPSK FSO communication system based on CML. The system is composed of three components, a CML-based modulator-free variable multi-rate RZ-DPSK signal transmitter, a self-coherent receiver, and optical antennas, as shown in Fig. 3(a). At the transmitter terminal, a Finisar DM80-01 CML is used, which has a maximum threshold current of 25 mA and an input impedance of 50 Ohms. To suppress the transient chirp of the CML in the experiment, the supply voltage of the CML is 3.57 V and the current is 71.4 mA, which is about 3 times the maximum threshold current. For simplicity, we pre-mapped pseudorandom bit sequence (PRBS) into a tri-level signal based on the rule that the CML generates RZ-DPSK modulation format, and loaded it into an arbitrary waveform generator (AWG). Then, the tri-level electrical signal is amplified to drive the CML to generate RZ-DPSK optical signals. In addition, considering the large channel attenuation and coupling loss, the modulated RZ-DPSK optical signal power is not enough to support the power requirements of FSO communication. Therefore, a high-power erbium-doped fiber amplifier (EDFA) is used to enhance the power of the RZ-DPSK optical signal. And the amplified signal is coupled to the transmitting optical antenna with a diameter of 2.5 cm through fiber. To evaluate the system performance at different received power, a variable optical attenuator (VOA) is added behind the high-power amplifier at the transmitter terminal to adjust the transmit power.

At the receiver terminal, the RZ-DPSK optical signal received by the optical antenna is very weak and needs to be amplified with a low-noise preamplifier and filter before being demodulated. The RZ-DPSK signal is demodulated by a spatial structure MZI with a free spectral range (FSR) of 2.5 GHz and a balanced photoreceiver with 3 dB bandwidth of 33 GHz. Finally, the data and clock are recovered by the clock and data recovery (CDR) circuit and the BER is measured by a signal quality analyzer. Fig. 3(b) and Fig. 3(c) show a scene diagram at the transmitter terminal and receiver terminal during the experiment, respectively. The transmitter and receiver are arranged in two buildings over 1 km, as shown in Fig. 4. And detailed experimental parameters are listed in Table I.

IV. Results and Discussion

A. Signal Modulation

Fig. 5(a) shows the spectrum of the generated RZ-DPSK signals with different transmission rates using an optical spectrum analyzer (OSA, YOKOGAWA AQ6370) with a resolution of 0.02 nm, which has an optical signal-noise ratio (OSNR) greater than 50 dB. The average power and center wavelength of the 2.5(5) Gbps RZ-DPSK signal were measured as −0.29(−0.15) dBm and 1552.062(1552.062) nm, respectively. Meanwhile, we also measured the phase noise and relative intensity noise (RIN) of the CML, the instantaneous linewidth of the CML is 2.29 MHz, and the RIN is −110 dBc/Hz @ 10 KHz.

TABLE I
EXPERIMENTAL PARAMETERS

Specifications		Value	Unit
Chirp-managed Laser	wavelength	1552.062	nm
	linewidth	2.29	MHz
	RIN	-110 @ 10 KHz	dBc/Hz
	frequency efficiency	0.24	GHz/mA
Mach-Zehnder interferometer	FSR	2.5	GHz
Rate		2.5/5	Gbps
Distance		1	km
Receiving/ Transmitting antenna diameter		2.5	cm
Transmitting power		adjustable	dBm

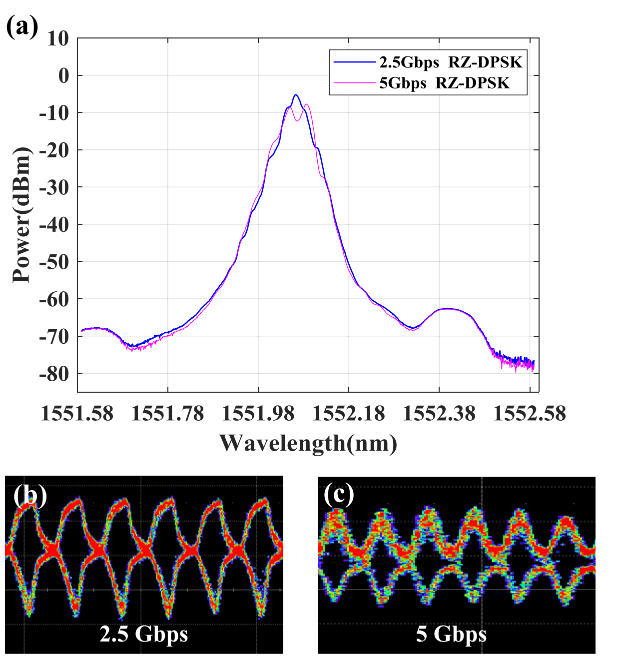

Fig. 5. (a) Optical spectrum of RZ-DPSK signals with different transmission rates. (b) Eye diagram of 2.5 Gbps RZ-DPSK at the transmitter terminal. (c) Eye diagram of 5 Gbps RZ-DPSK at the transmitter terminal.

To have a clear comparison of the signal quality at the receiving terminal, Fig. 5(b) and (c) show the measured eye diagrams obtained from direct demodulation of the optical signal without spatial transmission, which were measured by a 25 GHz serial data analyzer (SDA, LeCroy SDA 825Zi-A) with 20s persistence aging. The optical spectrum and eye diagram were measured at point A in Fig. 3(a). It can be noticed from the eye diagram that the quality of the generated 2.5 Gbps signal is better than that of 5 Gbps due to the low frequency efficiency (0.24 GHz/mA) of the CML.

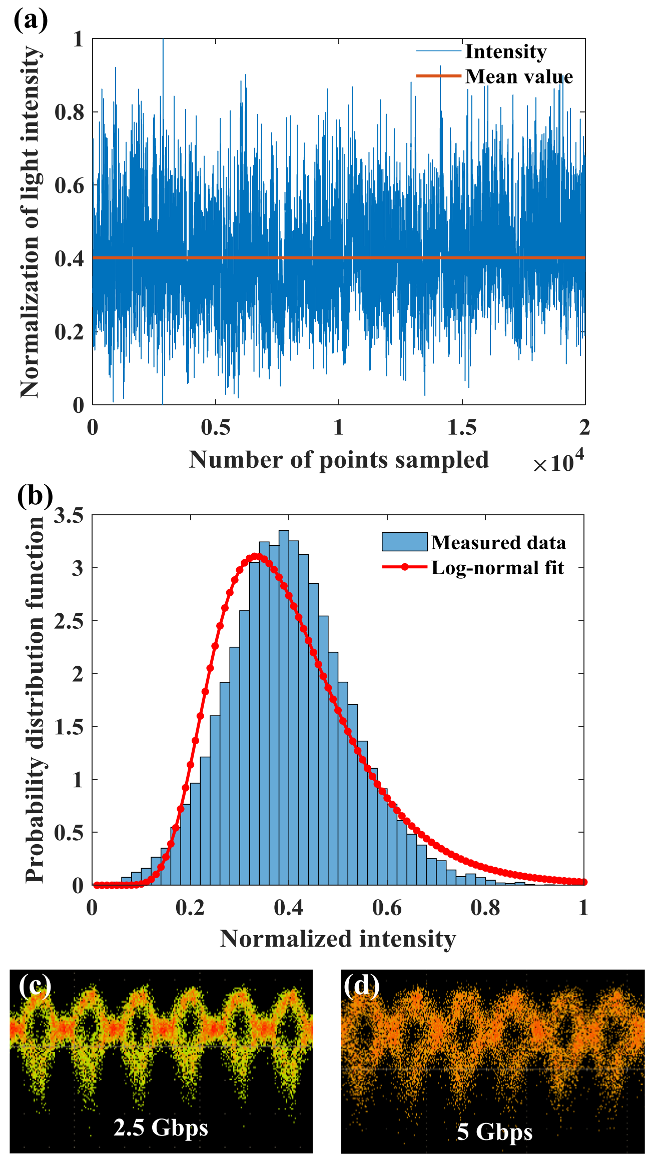

Fig. 6. **(a)** The normalized received light intensity. (b) Probability distribution function of the received light intensity. (c) Eye diagram of 2.5 Gbps RZ-DPSK at the receiver with BER of 1×10^{-3}. (d) Eye diagram of 5 Gbps RZ-DPSK at the receiver with BER of 1×10^{-3}.

B. Signal Demodulation

At the receiver terminal, the optical signal collected by the optical antenna was coupled into the optical fiber, after a low-noise amplifier, gaussian filter, and VOA, and then was fed into the MZI followed by a balanced photoreceiver for differential detection. In addition, a voltage of 2.47 V was applied to the phase tuning port of the MZI for optimum self-differential demodulation, which can maximize the output signal amplitude. During the communication test, we measured the light intensity fluctuation of the experimental environment, as shown in Fig. 6(a), which shows the normalized received light intensity variation over a period of time (20000 sampling points, 10ms sampling interval). Based on this, the scintillation index (σ_I^2) and the refractive index structure constant (C_n^2) [17] was obtained

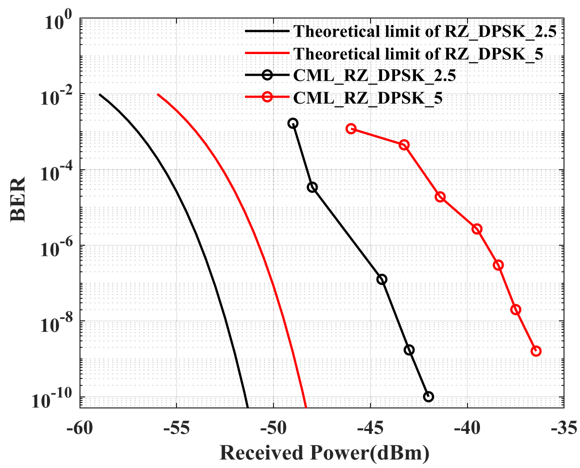

Fig. 7. Measured BERs as functions of the received power.

to be $\sigma_I^2 = 0.1$ and $C_n^2 = 9.13 \times 10^{-15}$. And the atmospheric turbulence distribution with a nearly Log-normal distribution was obtained by fitting to the probability density histogram, as shown in Fig. 6(b). The eye-diagram of RZ-DPSK at the receiver with BER of 1×10^{-3} was measured with a 23 GHz digital phosphor oscilloscope (Tektronix, DPO72304DX), as shown in Fig. 6(c) and (d).

Finally, the BER of the proposed system was measured using a signal quality analyzer (Anritsu MP1800A) at the receiver terminal to evaluate the communication performance. Fig. 7 shows the BER curves of 2.5 Gbps and 5 Gbps RZ-DPSK as a function of received power, and including the theoretical limit [18]. The required power for the CML RZ-DPSK is −48.9 dBm and −45.6 dBm at BER of 1×10^{-3}, corresponding to 2.5 Gbps and 5 Gbps, which indicates that the proposed modulator-free variable rate RZ-DPSK laser communication system can be achieved with excellent communication performance. The proposed scheme has a great advantage for SWaP-constrained communication platforms (e.g., satellite) because signal generation can be done without modulators. Another advantage of the proposed scheme is that it can provide communication for mobile platforms with a large dynamic range of power. As shown in Fig. 7, the BER curves show an increase of 3.3 dB in receiver sensitivity at 2.5 Gbps compared to 5 Gbps data rate at BER of 1×10^{-3}, which predicts that the communication link distance becomes 1.4 times than the original one. The increase in sensitivity is due to the increase in the average power per bit of energy as the rate decreases. Increased sensitivity can be translated into an increase in link margin, which allows the laser communication system to adapt to the situations of constantly changing link distances and channel conditions. It is worth emphasizing that the proposed system can generate RZ-DPSK signals at arbitrary rates depending on the rate of the tri-level signal. In the outfield experiments, limited by the FSR of MZI, we only performed outfield experiments at 2.5 Gbps and 5 Gbps rates.

In addition, we also analyze the gap between the experimental results and the theoretical BER curves for our subsequent improvement. For an FSO communication system, the signal quality will suffer deterioration due to background radiation, atmospheric scattering, and scintillation or beam drift caused by atmospheric turbulence [17], [19], which can lead to data loss and increased transmission BER. Furthermore, the stability of the optical antenna, and the noise of the amplifier also influence the signal quality, which consequently degrades the communication performance [20], [21]. Subsequently, we will consider implementing adaptive optics systems to eliminate the effect of atmospheric turbulence, thereby improving the stability of the system.

V. Conclusion

To miniaturize the FSO communication terminals and provide flexible and agile operation in the situations of constantly changing link distances and channel conditions, we have proposed and successfully carried out a demonstration of a CML-based modulator-free variable multi-rate RZ-DPSK FSO communication system with a space distance of 1 km, achieving the receiving sensitivity of −48.9 dBm and −45.6 dBm at BER of 1×10^{-3}, corresponding to 2.5 Gbps and 5 Gbps. Our experimental results verify the feasibility of the proposed system, and provide a novel idea for designing variable multi-rate FSO communication systems, which can help communication applications to achieve stable data transmission links over a large dynamic range of power. We believe that the proposed scheme can provide a valuable reference for FSO communication.

Acknowledgment

The authors sincerely thank the reviewers for their careful reading and valuable suggestions and declare no conflicts of interest.

References

[1] D. Powell, “Lasers boost space communications,” *Nature*, vol. 499, no. 7458, pp. 266–267, Jul. 2013, doi: 10.1038/499266a.
[2] H. Hemmati, *Near-Earth Laser Communications,* 2nd ed. Boca Raton, FL, USA: CRC Press, 2020.
[3] T. Wang et al., “Blimp-borne laser communication technology based on space dynamic base station,” *IEEE Photon. J.,* vol. 13, no. 5, Oct. 2021, Art. no. 7900107, doi: 10.1109/JPHOT.2021.3103426.
[4] K. P. Peppas and P. T. Mathiopoulos, “Free-space optical communication with spatial modulation and coherent detection over H-K atmospheric turbulence channels,” *J. Lightw. Technol.*, vol. 33, no. 20, pp. 4221–4232, Oct. 2015, doi: 10.1109/JLT.2015.2465385.
[5] V. W. S. Chan, “Optical satellite networks,” *J. Lightw. Technol.*, vol. 21, no. 11, pp. 2811–2827, Nov. 2003, doi: 10.1109/JLT.2003.819534.
[6] D. Gao et al., “Development current status and trend analysis of satellite laser communication (invited),” *Acta Photonica Sinica,* vol. 50, no. 4, pp. 9–29, Aug. 2021, doi: 10.3788/gzxb20215004.0406001.
[7] W. H. Gunawan et al., “Digital domain power division multiplexing optical OFDM for free space optical communication (FSOC) using 10-GHz bandwidth optical components,” *IEEE Photon. J.,* vol. 14, no. 4, Aug. 2022, Art. no. 7336707, doi: 10.1109/JPHOT.2022.3182867.
[8] D. Cornwell, “Space-based laser communications break threshold,” *Opt. Photon. News*, vol. 27, no. 5, pp. 24–31, May 2016, doi: 10.1364/OPN.27.5.000024.
[9] M. Toyoshima, “Recent trends in space laser communications for small satellites and constellations,” *J. Lightw. Technol.*, vol. 39, no. 3, pp. 693–699, Feb. 2021, doi: 10.1109/JLT.2020.3009505.
[10] H. Hauschildt et al., “Global quasi-real-time-services back to Europe: EDRS global,” in *Proc. Int. Conf. Space Opt.*, Chania, Greece, Jul. 2019, pp. 353–357, doi: 10.1117/12.2535952.

[11] W. Jia, J. Xu, Z. Liu, K.-H. Tse, and C.-K. Chan, "Generation and transmission of 10-Gb/s RZ-DPSK signals using a directly modulated chirp-managed laser," *IEEE Photon. Technol. Lett.*, vol. 23, no. 3, pp. 173–175, Feb. 2011, doi: 10.1109/LPT.2010.2092761.

[12] M. Shirasaki, H. Nishimoto, T. Okiyama, and T. Touge, "Fibre transmission properties of optical pulses produced through direct phase modulation of DFB laser diode," *Electron. Lett.*, vol. 24, no. 8, pp. 486–488, Apr. 1988, doi: 10.1049/el:19880330.

[13] A. S. Karar, Y. Gao, K. P. Zhong, J. H. Ke, and J. C. Cartledge, "Generation and transmission of DPSK signals using a directly modulated passive feedback laser," *Opt. Exp.*, vol. 20, no. 26, pp. B151–B158, Dec. 2012, doi: 10.1364/OE.20.00B151.

[14] J. Franklin et al., "Generation of RZ-DPSK using a chirp-managed laser (CML)," in *Proc. Conf. Opt. Fiber Commun./Nat. Fiber Optic Engineers Conf.*, San Diego, CA, USA, Feb. 2008, pp. 1–3. doi: 10.1109/OFC.2008.4528223.

[15] F. Fan and D. Mahgerefteh, "Chirp managed lasers: A new technology for 10 Gbps optical transmitters," *Optik Photonik*, vol. 2, no. 4, pp. 39–41, Dec. 2007, doi: 10.1002/opph.201190284.

[16] D. Mahgerefteh, Y. Matsui, X. Zheng, and K. McCallion, "Chirp managed laser and applications," *IEEE J. Sel. Topics Quantum Electron.*, vol. 16, no. 5, pp. 1126–1139, Sep. 2010, doi: 10.1109/JSTQE.2009.2037336.

[17] A. Tunick, "Optical turbulence parameters characterized via optical measurements over a 2.33 km free-space laser path," *Opt. Exp.*, vol. 16, no. 19, pp. 14645–14654, Sep. 2008, doi: 10.1364/OE.16.014645.

[18] G. P. Agrawal, *Fiber-Optic Communication Systems*, 4th ed., Hoboken, NJ, USA: Wiley, 2010, ch. 10.

[19] R. K. Singh, Karmeshu, and S. Kumar, "A novel approximation for K distribution: Closed-form BER using DPSK modulation in free-space optical communication," *IEEE Photon. J.,* vol. 9, no. 5, Oct. 2017, Art. no. 7906814, doi: 10.1109/JPHOT.2017.2746763.

[20] H. Jian, D. Ke, L. Chao, Z. Peng, J. Dagang, and Y. Zhoushi, "Effectiveness of adaptive optics system in satellite-to-ground coherent optical communication," *Opt. Exp.*, vol. 22, no. 13, pp. 16000–16007, Jun. 2014, doi: 10.1364/OE.22.016000.

[21] J. Chen et al., "Free-space communication turbulence compensation by optical phase conjugation," *IEEE Photon. J.,* vol. 12, no. 5, Oct. 2020, Art. no. 7905611, doi: 10.1109/JPHOT.2020.3024220.